

Electrophysiological Characterization of Benzofuroindole-Induced Potentiation of Large-conductance Ca^{2+} -activated K^{+} Channels

Tal Soo Ha¹, Hyun-Ho Lim, Ga Eun Lee, Yong-Chul Kim, and Chul-Seung Park

Department of Life Science, Gwangju Institute of Science and Technology (GIST), Gwangju, Korea

Running title: Mechanism of a BK_{Ca} channel activator

Corresponding author: Chul-Seung Park, Ph.D.

Department of Life Science

Gwangju Institute of Science and Technology

1 Oryong-dong, Buk-gu, Gwangju, 500-712, Korea

TEL: 82-62-970-2489

FAX: 82-62-970-2484

cspark@gist.ac.kr

¹Current address: Department of Pharmacology and Center for Basic Neuroscience, University of Texas Southwestern Medical Center, Dallas, TX, USA

Number of text pages: 29 pages

Number of tables: none

Number of figures: 5 figures

Number of references: 31 references

Number of words in Abstract: 176 words

Number of words in Introduction: 546 words

Number of words in Discussion: 654 words

List of nonstandard abbreviations: BK_{Ca}, Large-conductance Ca²⁺-activated K⁺ channels; TBIC, 7-trifluoromethyl-10*H*-benzo[4,5]furo[3,2-*b*]indole-1-carboxylic acid; rSlo, rat BK_{Ca} channel α subunit; h β 1, human β 1 subunit of BK_{Ca} channel; r β 4, rat β 4 subunit of BK_{Ca} channel.

ABSTRACT

Large-conductance Ca^{2+} -activated K^+ (BK_{Ca}) channels are widely distributed and play key roles in various cell functions. We previously reported the chemical synthesis of several benzofuroindole compounds that act as potent openers of BK_{Ca} channels. In this study, we investigated the mechanism of channel potentiation by one of the compounds, 7-trifluoromethyl-10*H*-benzo[4,5]furo[3,2-*b*]indole-1-carboxylic acid (TBIC), using electrophysiological means. The chemical highly activated cloned BK_{Ca} channels from extracellular side independent of β subunits and regardless of the presence of intracellular Ca^{2+} . The EC_{50} and Hill coefficient for rat BK_{Ca} channel α subunit, rSlo, were estimated as $8.9 \pm 1.5 \mu\text{M}$ and 0.9, respectively. TBIC shifted the conductance-voltage curve of rSlo channels to more hyperpolarized potentials without altering its voltage dependence. Single-channel recording revealed that TBIC increased the open-probability of the channel in a dose-dependent manner without any changes in single-channel conductance. Strong potentiation by TBIC was also observed for native BK_{Ca} channels from rat hippocampus pyramidal neurons. Thus, TBIC and the related benzofuroindole compounds can be useful tools to unravel the mechanism of this novel allosteric activation of BK_{Ca} channels.

INTRODUCTION

Large-conductance Ca^{2+} -activated K^+ channels (BK_{Ca} or Maxi-K channels) are a family of potassium-selective ion channels activated in response to membrane depolarization and are modulated by intracellular concentration of Ca^{2+} (for review, Toro et al., 1998; Weiger et al., 2002). These channels are widely expressed in many different types of both excitable and non-excitable cells. They have significant physiological roles in regulation of frequency of firing, action potential afterhyperpolarization, and neurotransmitter release (Vergara et al., 1998; Kaczorowski and Garcia, 1999). Their activities play a pivotal role in the negative feedback control of intracellular Ca^{2+} concentration and protect neuronal cells from excess Ca^{2+} influx through the voltage-dependent Ca^{2+} channels during pathophysiological environments (Lawson, 2000). In hyperactive neuronal cells, activation of BK_{Ca} channels is thought to be required for restoring resting membrane potential by down-regulating the activity of voltage-dependent Na^+ and Ca^{2+} channels (Jaggar et al., 2000; Brenner et al., 2000). In addition, activation of BK_{Ca} channel significantly contributes to action potential repolarization and afterhyperpolarization during excitation-contraction coupling in smooth muscle cells (Ohi et al., 2001).

For these reasons, BK_{Ca} channel openers may be effective in protecting neuronal cells from damage during or after ischemic stroke and in down-regulating hyperactivity in smooth muscle cells (for review, Shieh et al., 2000). BK_{Ca} channels are composed of two different subunits, the pore-forming α subunit and the auxiliary β subunits. While channels formed only by four α subunits can be functional, β subunits alter the biophysical and pharmacological properties of homomeric channels including Ca^{2+} and voltage sensitivity, and gating kinetics (Valverde et al., 1999; Wallner et al., 1999; Xia et al., 1999; Qian et al., 2002; Ha et al., 2004). Several compounds have been developed and reported to be BK_{Ca} channel openers, e.g., dehydrosoyasaponin-I, maxikdiol, NS-

1619, BMS-204352, 17 β -estradiol, ethylbromide tamoxifen, pimaric acid, and epoxyeicosatrienoic acids (Coghlan et al., 2001; Imaizumi et al., 2002; Dick et al., 2002; Valverde et al., 1999; Vergara et al., 1998). While some synthetic activators such as NS-1619 and BMS-204352 act on the α subunit, other openers of BK_{Ca} channels including dehydrosoyasaponin-I and 17- β -estradiol require β subunit for their action (Giangiacomo et al., 1998; Valverde et al., 1999). Several activators derived from natural products such as dehydrosoyasaponin-I are impermeable to the cell membrane and act only on intracellular side of BK_{Ca} channels (Kaczorowski and Garcia, 1999).

Benzofuroindole analogs were shown to relax smooth muscles of bladder possibly via the activation of BK_{Ca} channels (Butera et al., 2001). In our previous study, we reported the chemical synthesis of new benzofuroindole derivatives and the screening for their efficacy on cloned BK_{Ca} channels expressed in *Xenopus* oocytes (Gormemmis et al., 2005). One of the initial compounds, referred as 'compound 8', highly up-regulated the activity of BK_{Ca} channels. In the present study, we further investigated this compound, 7-trifluoromethyl-10*H*-benzo[4,5]furo [3,2-*b*]indole-1-carboxylic acid (TBIC) (Fig. 1, *inset*), in order to reveal its mechanism of action with respect to channel activation. We found that TBIC activated BK_{Ca} channel in a dose-dependent manner at micromolar concentration from extracellular side and its activation was independent of β subunits. TBIC shifted the conductance-voltage relationship of the channel to more hyperpolarized potentials without altering voltage dependence. In addition, single-channel analysis showed that the compound increased the open-probability (P_o) of the channel by altering gating kinetics without affecting its single-channel conductance.

MATERIALS AND METHODS

Functional expression of cloned BK_{Ca} channel subunits in Xenopus oocytes

The complementary DNAs (cDNAs) of rat BK_{Ca} channel α subunit (*rSlo*), human β 1 subunit (*h β 1*), and rat β 4 subunit (*r β 4*) were subcloned into pGH vector for expression in *Xenopus* oocytes. The sequence information of rSlo, h β 1, and r β 4 used in this study can be obtained from GenBank with the accession numbers of AF135265 (Ha et al., 2000), NM004137 (Meera et al., 1996), and AY028605 (Ha et al., 2004), respectively. Each cDNA was subcloned into pGH expression vector containing the 5'- and 3'-untranslated regions of *Xenopus* β -globin gene, since it is known to enhance the protein expression of certain mammalian messages in *Xenopus* oocytes (Liman et al., 1992). Complementary RNA (cRNA) of each construct was prepared *in vitro* as described in previous studies (Ha et al., 2000; 2004). Plasmid DNA was purified (Qiagen midi-prep columns, Qiagen, Valencia, CA) and digested with a restriction enzyme, NotI. RNA was synthesized from linearized plasmid DNA using T7 RNA polymerase in the presence of a cap analog, m⁷G(5')ppp(5')G, and NTPs. Oocytes of stage V-VI were surgically removed from the ovarian lobes of anesthetized female *Xenopus laevis* (Xenopus One, Dexter, MI) and transferred into Ca²⁺-free OR medium (86 mM NaCl, 1.5 mM KCl, 2 mM MgCl₂, 10 mM HEPES, 50 μ g/ml gentamycin [pH7.6]). The follicular cell layer was removed by incubating oocytes in Ca²⁺-free OR medium containing 3 mg/ml collagenases (Worthington Biochemical, NJ) for 2 hours. The oocytes were then washed extensively with and kept in ND-96 medium (96 mM NaCl, 2 mM KCl, 1.8 mM CaCl₂, 1 mM MgCl₂, 5 mM HEPES, and 50 μ g/ml gentamicin at pH7.6) at 18 °C. Each oocyte was injected with 50 nl containing approximately 1 ng of cRNA for single-channel and 50 ng for macroscopic current recordings, respectively, using a microdispenser (Drummond, Broomall, PA). Injected oocytes were incubated at 18 °C for 3-5 days in sterile ND-96 medium.

Immediately prior to patch-clamp experiments, the vitelline membrane was removed manually with fine forceps.

Primary culture of pyramidal neurons in rat hippocampus

Primary culture of rat hippocampal pyramidal neuron has been described previously (Abdel-Hamid and Baimbridge, 1997). Sprague-Dawley rats were anesthetized and decapitated at embryonic day 18. The hippocampus was surgically dissected and isolated from fetal brain and minced in Ca^{2+} , Mg^{2+} -free Hank's balanced salt solution (HBSS, Invitrogen, Carlsbad, CA). The tissue was digested with 0.1 % trypsin-EDTA to the medium and then stopped by adding the same volume of fetal bovine serum. Cell dissociation was accomplished by gentle mechanical agitation. After removing cell debris by centrifugation for 2 min, the cell pellet was resuspended in minimum essential medium (MEM, Invitrogen) with 10 % of a 1:1 mixture of heat-inactivated horse and fetal bovine serum. The dissociated cells were plated on 35-mm tissue culture dishes (Falcon, Franklin Lakes, NJ) coated with poly-L-lysine (Sigma-Aldrich, St.Louis, MO). The cells were incubated at 37 °C in a humidified, 5 % CO_2 incubator. The medium was renewed after 24 hrs and half-exchanged twice a week with feeding media. The feeding media contained apo-transferrin (200 $\mu\text{g}/\text{ml}$, Sigma-Aldrich), insulin (1 $\mu\text{g}/\text{ml}$, Sigma-Aldrich), sodium selenite (30 nM, Sigma-Aldrich), putrescine (100 μM , Sigma-Aldrich), progesterone (20 μM , Sigma-Aldrich), 5 % equine serum (HyClone, Logan, UT), and MEM (Invitrogen). The cultured neurons were used for electrophysiological recording during 12-18 days in culture.

Electrophysiological recordings and data analysis

All single-channel and macroscopic current recordings were performed using gigaohm-seal patch-clamp method in either excised inside-out or outside-out configuration (Hamil et al.,

1981). Patch pipettes were fabricated from borosilicate glass (WPI, Sarasota, FL) and fire-polished to the resistance of 2-5 M Ω for macroscopic patches and 5-8 M Ω for single-channel recording, respectively. For single-channel recordings, patch pipettes were coated with beeswax to reduce electrical noises. The channel currents were amplified using an Axopatch 200B amplifier (Axon Instruments, Foster City, CA), low-pass filtered at 1 or 2 kHz using a four-pole Bessel filter, and digitized at a rate of 10 or 20 points/ms using a Digidata 1200A (Axon Instruments). No series resistance compensation was used and linear leak currents were subtracted from macroscopic currents.

In recording rat hippocampal neurons, pyramidal cells were distinguished from mixed population including glia by morphological features. Prior to electrophysiological recording, the culture medium was washed multiple times with Na⁺-saline solution containing 140 mM NaCl, 4 mM KCl, 0.24 mM KH₂PO₄, 2 mM MgCl₂, 2 mM CaCl₂, 10 mM D-glucose, and 10 HEPES (pH 7.4). Cells were then rinsed in symmetrical 124 mM K⁺ solution for recordings. Patch recordings were made from the soma of cultured pyramidal neurons in the outside-out patch configuration at room temperature. From a total of 76 patches in neuron cells, 22 recordings showed single-channel level activities of BK_{Ca} channels

Single rSlo or native BK_{Ca} channels were readily activated at high concentration of intracellular Ca²⁺ and by briefly delivered membrane potentials to 100 mV. For single-channel analysis, transitions between closed and open states were determined by setting the threshold at half of the unitary current-amplitude. To determine the single-channel conductance of expressed channels, mean-amplitudes of channel currents were obtained from histograms fitted with Gaussian distributions and the mean currents were plotted against transmembrane voltages. Slope-conductance values were obtained from linear regression.

Macroscopic currents of expressed channels were activated by voltage-clamp pulses delivered from a holding potential, -50 mV for [Ca²⁺]_i at 0 μ M, -100 mV at 1 μ M, and -150 mV at

5 μ M, respectively, to membrane potentials ranging usually from -150 to 200 mV in 10 mV or 20 mV increments. Solutions for both single and macroscopic channels recordings contained gluconates as a nonpermeant anion to prevent the activation of endogenous calcium-activated chloride channels. The intracellular and extracellular solutions contained the following components unless specified otherwise (in mM): 120 potassium gluconate, 10 HEPES, 4 KCl, and 5 EGTA, pH 7.2 . In order to provide required free $[Ca^{2+}]_i$, the appropriate amount of total Ca^{2+} to add to the intracellular solution was calculated using a program, MaxChelator (Patton et al. 2004; <http://www.stanford.edu/~cpatton/maxc.html>). To compare the of the channel characteristics accurately, an identical set of intracellular solutions was used throughout the entire experiments. Commercial software packages, such as Clampex 8.0 or 8.1 (Axon instruments) and Origin 6.1 (OriginLab, Northampton, MA), were used for the acquisition and the analysis of both single-channel and macroscopic recording data.

Reagents

The chemical synthesis of 7-trifluoromethyl-10*H*-benzo[4,5]furo[3,2-*b*]indole-1-carboxylic acid (TBIC) was described in a previous study where the compound was referred to as ‘compound 8’ (Gormemis et al., 2005). TBIC was dissolved in DMSO (Sigma-Aldrich) in 500 mM stock solutions and stored at -20 °C until the usage. All reagents, buffered in bath solution to pH 7.2 , were applied directly to membrane patches by gravity perfusion with 10 volumes of recording chamber at a flow rate of $1-2$ ml/min.

Statistical Analysis

All data were presented as means \pm standard error of mean (S.E.M.), where n indicates the number of independent experiments. For each data set, the statistical significance of the

difference was tested using ANOVA for independent observations. In all cases, $P < 0.05$ was considered significant. Each macroscopic current trace represents an average of three records in succession.

RESULTS

Effects of a benzofuroindole, TBIC, on macroscopic currents of a cloned BK_{Ca} channel expressed in Xenopus oocytes

To understand the potentiation mechanism of TBIC on BK_{Ca} channel, we first characterized its effects on macroscopic currents of rat BK_{Ca} channel α subunit (rSlo) expressed in *Xenopus* oocytes. In Fig. 1, the time-dependent effects of TBIC were monitored from a membrane patch containing hundreds of rSlo channels by applying 50 ms step-pulses to 50 mV every second. Small rSlo currents were initially evoked by the voltage-pulses (Fig. 1a), since the intracellular (pipette) solution contained only 0.5 μ M Ca²⁺. When 20 μ M of TBIC was applied on to the extracellular side of membrane patch, a large increase in the rSlo currents was observed. The full potentiation was achieved in two phases: the initial fast-activation occurring within 10 seconds (Fig. 1b) and the following slower-phase over a few minutes (Fig. 1c). Upon cessation of TBIC application, the channel activity rapidly decreased within in 10 s, (Fig. 1d). In some cases, the channel activity did not return fully to the pre-treatment level and a slight increase in channel activity remained (Fig. 1, a and d). However, the fast on-set and off-set of TBIC effects in cell-free recording condition suggest strongly that the compound interacts directly to the channel from extracellular side and enhance its activity.

Concentration-dependence of TBIC on macroscopic rSlo channels and effects of β -subunits

We then determined the concentration-dependence of TBIC on macroscopic rSlo currents. As increasing concentrations of TBIC were applied to the extracellular side of membrane patches, the activation rate as well as the level of steady-state current were increased in a concentration-dependent manner (Fig. 2 A). To compare the effects of TBIC measured at specific concentrations,

we normalized the ionic currents in the presence of a given concentration of TBIC (I) with the current in the absence of TBIC (I_0). The relative fold-increase (I / I_0) were plotted against the concentration of TBIC and fitted with a Hill equation (Fig. 2 A, right panel). Although we were not able to obtain the concentration of TBIC higher than 300 μ M due to its solubility in water, we noticed that TBIC-induced current increases reached plateau levels at around 100 μ M (Fig. 2 A). The half-effective concentration (EC_{50}) and Hill coefficient (n), were obtained by fitting individual titration data to Hill equation (the legend of Figure 2), and the statistical means and standard errors were calculated using the values obtained from more than three independent experiments. The EC_{50} and Hill coefficient (n) of extracellular TBIC for rSlo channel were determined as 8.9 ± 1.5 μ M and 0.9 ± 0.1 , respectively (Fig. 2 A, *filled circles*, $n = 5$). We also measured the effects of TBIC using inside-out patch configuration to determine whether this compound also affects channel activity from intracellular side. The intracellular Ca^{2+} concentration was fixed at 2 μ M to activate rSlo channels and different concentrations of TBIC were added to the intracellular side of the membrane. Although intracellular TBIC also increased rSlo currents with a similar apparent affinity, EC_{50} of 12.7 ± 5.8 μ M, its fold-increase was much smaller than that obtained from extracellular side (Fig. 2 A, *filled squares*, $n = 3$).

The functional characteristics of BK_{Ca} channels are altered by auxiliary β subunits, and the efficacy of some activators and inhibitors are greatly influenced by co-assembly of β subunits. Thus, we asked whether the potentiating effects of TBIC are affected by co-expression of β subunits. We expressed rSlo together with either human $\beta 1$ or rat $\beta 4$ subunit in *Xenopus* oocytes and measured the channel currents in the presence of different concentrations of extracellular TBIC. We usually used 12-fold molar excess of the h $\beta 1$ and r $\beta 4$ transcripts to ensure the sufficient co-assembly of β subunits with rSlo subunit. The activities of both rSlo/h $\beta 1$ (Fig. 2 B, $n = 4$) and rSlo/r $\beta 4$ (Fig. 2C, $n = 4$) were increased by micromolar concentration of the compound in a

concentration-dependent manner. EC_{50} values of extracellular TBIC were determined as $10.0 \pm 1.5 \mu\text{M}$ for rSlo/h β 1 heteromeric channels (Fig. 2B, *filled triangle*) and $4.5 \pm 0.7 \mu\text{M}$ for rSlo/r β 4 heteromeric channels (Fig. 2C, *filled diamond*) with Hill coefficients of 0.7 ± 0.1 and 1.1 ± 0.2 , respectively, indicating that minor but statistically significant differences in both the apparent affinity and the cooperativity of TBIC were brought about by the co-expression of different β subunits. However, these results indicate that TBIC can potentiate BK_{Ca} channel without the co-assembly of β subunits and argue that the receptor site of TBIC locates within the main subunit of BK_{Ca} channel, the Slo protein.

Efficacy of extracellular TBIC in different concentrations of intracellular Ca^{2+}

Since the activity of BK_{Ca} channels are modulated by intracellular Ca^{2+} , we wondered how intracellular Ca^{2+} interplay the action of TBIC from extracellular side and whether TBIC can activate channel in the complete absence of intracellular Ca^{2+} .

In Figure 3A, we tested the effects of extracellular TBIC at two different concentrations in the absence of intracellular Ca^{2+} . To keep $[\text{Ca}^{2+}]_i$ at sub-nanomolar range, 5 mM EGTA was supplemented into the intracellular pipette solution. Even in the absence of intracellular Ca^{2+} , the activation of rSlo channels was observed at extreme positive voltages, greater 100 mV (*top row*, Control). The application of 30 μM extracellular TBIC greatly potentiated the channel activity and large outward currents were measured (*top row*, 30 μM [TBIC]_o). As illustrated in the current-voltage (*I-V*) relationship (*top row*, *right panel*), TBIC shifted the threshold voltage of channel activation to less positive voltages and the channel currents were observed at voltage as low as 60 mV in 30 μM TBIC (*empty circles*). In the presence of 100 μM TBIC, *I-V* relationship of rSlo channel was further shifted and the currents were activated near 20 mV (*empty triangles*). Robust outward currents were consistently recorded at the membrane voltages greater than 20 mV. In the

presence of 1 μM $[\text{Ca}^{2+}]_i$, 30 μM TBIC also shifted the I - V relationship to less positive voltages and large tail currents evoked by rSlo were observed (*middle row*, 30 μM $[\text{TBIC}]_o$). Since the channels were activated near -60 mV in the presence of 100 μM TBIC, we were able to detect inward currents at negative test-voltages (*middle row*, 100 μM $[\text{TBIC}]_o$ and *half-filled triangles* in *right panel*). Inward currents were even more dramatic when $[\text{Ca}^{2+}]_i$ was increased to 5 μM (Fig. 3A, *bottom row*). With the treatment of 30 μM TBIC, the activation of rSlo channel became evident even at -100 mV and the peak inward K^+ currents was observed at around -40 mV (*filled circles*). The most impressive effect of TBIC was seen at 100 μM in the presence of 5 μM $[\text{Ca}^{2+}]_i$. rSlo channels were activated robustly from -130 mV and resulted in large inward currents peaked near -70 mV (*bottom row*, 100 μM $[\text{TBIC}]_o$ and *filled triangles* in *right panel*). It is intriguing that the linear I - V relationship, a characteristic of the BK_{Ca} channel, could be appreciated by measuring steady-state currents instead of instantaneous tail-currents.

The effects of TBIC on macroscopic rSlo channel were summarized in Figure 3 B and C. Sets of conductance-voltage (G - V) relationships and their half-activation voltages ($V_{1/2}$) were shown for four different concentrations of TBIC, 0 μM (*square*), 10 μM (*circle*), 30 μM (*triangle*), and 100 μM (*down triangle*), in the presence of three different concentrations of $[\text{Ca}^{2+}]_i$, 0 μM (*empty*), 1 μM (*half-filled*), and 5 μM (*filled*). The significant effects of TBIC on G - V relationship were observed at the concentrations higher than 1 μM and the further increase resulted in steady shifts in G - V curves toward the negative direction. While the addition of TBIC up to 100 μM shifted the G - V curve -134 mV, from 210 ± 7.5 mV to 76 ± 4.0 mV, in the absence of Ca^{2+} , a smaller shift of about -83 mV was observed by identical concentration of TBIC at 5 μM $[\text{Ca}^{2+}]_i$. Despite the large shifts in their positions, no significant change was detected in the steepness of G - V curves, the measure of voltage-dependence in channel activation, within a set of identical $[\text{Ca}^{2+}]_i$. These results indicate that BK_{Ca} channel can be activated by TBIC in the complete absence of intracellular

Ca^{2+} and that the potentiation is due to the shift of its voltage-activation profile to a more negative range without affecting its voltage sensitivity.

Effects of extracellular TBIC on single-channel currents of rSlo

To obtain further insights into the mechanism of action, the effects of TBIC were investigated at the single-channel level. For each outside-out patch, we depolarized the membrane voltage to more than 80 mV to significantly activate rSlo channels in order to count the number of channels in the membrane. Only those patches containing a single rSlo channel were used for subsequent experiments. Single-channel recordings were performed at various durations to obtain accurate values of steady-state kinetic constants: 5 to 8 min at hyperpolarized voltages and 0.5 to 2 min at depolarized voltages. Representative traces of a single rSlo channel in the absence and the presence of 20 μM TBIC were shown in Figure 4 A. The channel currents were recorded at 2 μM $[\text{Ca}^{2+}]_i$ at the specified membrane voltages. The opening of the channel was highly dependent on the membrane voltages as expected. The gating behavior, however, was dramatically altered by the application of 20 μM TBIC to the extracellular side (Fig. 4 A). While the rSlo channel rarely opens in control solution at -25 mV, the addition of 20 μM TBIC to extracellular side made the channel open readily. In addition, the open probability (P_o) was greatly increased at 25 mV by TBIC treatment. To examine the effects of TBIC on single-channel conductance, we measured the unitary current-amplitudes of rSlo at various membrane voltages in the absence and presence of TBIC, and the single-channel I - V relationships were plotted (Fig. 4B). Single-channel conductances were estimated as 246.1 ± 5.4 pS in control and 247.7 ± 4.2 pS in TBIC, respectively, indicating that the drug did not affect the single-channel conductance of rSlo. We then analyzed the effects of TBIC on single-channel P_o of the channel. Under control conditions, the increase in P_o was highly dependent on membrane voltage in the range of -75 mV and 25 mV and P_o values

were well fitted by a Boltzmann function (Fig. 4 C, *empty symbols*). The voltage required for half-maximum activation, $V_{1/2}$, was determined as 38.1 ± 3.1 mV. In the presence of 20 μ M TBIC, the P_o versus voltage curve shifted in a parallel manner to the negative direction by 33 mV and $V_{1/2}$ was estimated as 4.8 ± 3.4 mV. It is worth noting that the slopes of voltage activation curve remained unchanged, 0.031 for control currents and 0.035 for TBIC-potentiated currents, respectively. These results are in a good agreement with the previous findings in macroscopic rSlo currents, where the G - V curve was also shifted in parallel by TBIC, (Fig. 3B) further indicating that the potentiation of BK_{Ca} channel activity by TBIC is the direct result of the P_o increase.

Effects of TBIC on single BK_{Ca} channels of cultured hippocampus pyramidal neuron

Since BK_{Ca} channels in brain neurons are known to express as a heterogenous population due to extensive RNA splicing, co-assembly with $\beta 4$ subunit, and post-translation modifications, we wondered whether the activity of native neuronal BK_{Ca} channels could also be potentiated by TBIC. We thus performed outside-out patch recording on pyramidal neurons of rat hippocampus. Although in most instances more than one BK_{Ca} channels were observed in single patches, we were able to determine unambiguously the number of channels using brief depolarizing pulses. Representative current traces, obtained from a membrane patch containing four neuronal BK_{Ca} channels, were shown in Figure 5. Similar to the single-channel recordings of rSlo channel expressed in *Xenopus* oocytes (Fig. 4A), neuronal BK_{Ca} channel showed high single-channel conductances and steep voltage-dependence. Although extracellular treatment of 20 μ M TBIC highly increased the P_o of native BK_{Ca} channels at all membrane voltages tested, the effects were more dramatic for negative voltage ranges. While channel openings were observed only rarely in control solution containing 2 μ M $[Ca^{2+}]_i$ at -25 mV, the opening of all four BK_{Ca} channels were frequently observed in the presence of 20 μ M TBIC. The time-dependent effects of TBIC on

neuronal BK_{Ca} channels were compared at two different voltages, 25 and -25 mV (Fig. 5B and C). The P_o increase induced by TBIC treatment was almost instantaneous and readily reversible. Thus, we can conclude that this compound highly potentiates native BK_{Ca} channels from rat hippocampal neurons as well as the cloned rSlo channel.

DISCUSSION

In the present study, we characterized the effects of a benzofuroindole derivative, TBIC, on BK_{Ca} channels. This compound highly activates both native and cloned BK_{Ca} channels in a dose-dependent manner from the extracellular side of the membrane at low micromolar concentrations. TBIC potentiates the channel activity by shifting its P_o -voltage relationship to more negative voltages without affecting the single-channel conductance or the voltage sensitivity. However, the action of TBIC is non-cooperative and thus the dose-response curve of TBIC is best fitted with Hill coefficient of 1.

TBIC is a derivative of benzofuroindole with a carboxylic acid and a tri-fluoromethyl moiety at the position 1 and 7, respectively (Fig. 1, inset). In our previous study, we showed that a negative charge at the position 1 and a strong electron-withdrawing group at the position 7 are critical for the activity of TBIC (Gormemis et al., 2005). Since TBIC acts from extracellular side of the membrane and does not require β subunit for its action, we assume that the binding site of this negatively charged compound is in the extracellular region of the main subunit, Slo protein. Since the binding sites have not been identified for the previously known BK_{Ca} channel activators, especially those targeting the α subunit such as NS-1619 and BMS-204352 (for review, see Starrett et al., 1996; Coghlan et al., 2001), it is not clear at this point whether benzofuroindoles act on the identical site for their action. Thus, it is our desire to localize the receptor site for benzofuroindoles and to understand the molecular mechanism of this novel modulation. Slo protein, the α subunit of BK_{Ca} channel, has seven membrane-spanning regions (S0-S6) with an amino terminus of about 8 kDa and three loops facing the extracellular side of the membrane. Since β 1 subunit confers its potentating effect by interacting with the extracellular N-terminus and the first transmembrane helix, S0, it is conceivable that the TBIC may interact with the same region and activates the channel activity (Dick et al., 2001; Cox and Aldrich, 2000; Meera et al., 1997). It

remains to be seen whether the deletion of the N-terminal region removes the effect of TBIC. There has been much progress in predicting optimum binding site of a given compound based on detailed structure-activity relationship (Dick et al., 2001). The structure-activity profiles of benzofuroindole derivatives, reported in the previous studies (Butera et al., 2001; Gormemmis et al., 2005), can be utilized to predict the potential sites for TBIC on BK_{Ca} channel α subunit.

TBIC can activate native neuronal BK_{Ca} channels as well as the heterologously expressed Slo channels. At the single-channel level, the compound never failed to potentiate the BK_{Ca} channels in excised membrane of cultured neuron. We noticed that the potentiating effects of TBIC on neuronal BK_{Ca} channel might be even greater than those on cloned BK_{Ca} channel, although we were not able to quantify this precisely. This variability might be the result of the splicing variants of Slo or post-translational modification of BK_{Ca} channels in specific neurons. In a previous report, benzofuroindole derivatives were described to activate BK_{Ca} channels of smooth muscles only in rat bladder but not in arteries (Butera et al., 2001). Since the efficacy of TBIC was not significantly affected by different β subunits (Fig. 2 B and C), we wonder whether differential splicing of the Slo message affects the efficacy of TBIC on BK_{Ca} channels in different tissues. Thus, it will be important to assess the effects of TBIC in BK_{Ca} channels in different tissues and to correlate the efficacy with the nature of BK_{Ca} channels in the future.

In conclusion, our results provide the mechanistic details of benzofuroindole action on BK_{Ca} channel as a potentiator. Since TBIC and related compounds can activate BK_{Ca} channels so effectively, they can be used as experimental probes for a new allosteric site important for channel activation and be served as lead compounds for developing synthetic activators of BK_{Ca} channel for pharmaceutical purposes.

ACKNOWLEDGMENTS

The authors are grateful to the members of Laboratory of Molecular Neurobiology at GIST for valuable comments and timely help throughout the work, and to M. Walden at Brandeis University for his critical reading of the manuscript.

REFERENCE

Abdel-Hamid KM and Baimbridge KG (1997) The effects of artificial calcium buffers on calcium responses and glutamate-mediated excitotoxicity in cultured hippocampal neurons. *Neuroscience* **81**:673-687.

Brenner R, Perez GJ, Bonev AD, Eckman DM, Kosek JC, Wiler SW, Patterson AJ, Nelson MT and Aldrich RW (2000). Vasoregulation by the beta1 subunit of the calcium-activated potassium channel. *Nature* **407**:870-876.

Butera JA., Antane SA, Hirth B, Lennox JR, Sheldon JH, Norton NW, Warga D and Argentieri TM (2001) Synthesis and potassium channel opening activity of substituted 10H-benzo[4,5]furo[3,2-b]indole-and 5,10-dihydro-indeno[1,2-b]indole-1-carboxylic acids. *Bioorg Med Chem Lett* **11**:2093-2097.

Coghlan MJ, Carroll WA and Gopalakrishnan M (2001) Recent developments in the biology and medicinal chemistry of potassium channel modulators: update from a decade of progress. *J Med Chem* **44**:1627-1653.

Cox DH and Aldrich RW (2000) Role of the beta1 subunit in large-conductance Ca^{2+} -activated K^{+} channel gating energetics. Mechanisms of enhanced Ca^{2+} sensitivity. *J Gen Physiol* **116**:411-432.

Dick GM, Hunter AC and Sanders KM (2002) Ethylbromide tamoxifen, a membrane-impermeant antiestrogen, activates smooth muscle calcium-activated large-conductance potassium channels from the extracellular side. *Mol Pharmacol* **61**:1105-1113.

Dick GM, Rossow CF, Smirnov S, Horowitz B and Sanders KM (2001) Tamoxifen activates smooth muscle BK channels through the regulatory beta 1 subunit. *J Biol Chem* **276**:34594-34599.

Giangiacomo KM, Kamassah A, Harris G and McManus OB (1998) Mechanism of maxi-K

channel activation by dehydrosoyasaponin-I. *J Gen Physiol* **112**:485-501.

Gormemmis AE, Ha TS, Im I, Jung KY, Lee JY, Park CS and Kim YC (2005) Benzofuroindole analogues as potent BK_{Ca} channel openers. *Chembiochem* **6**:1745-1748.

Ha TS, Heo MS and Park CS (2004) Functional effects of auxiliary β 4 subunit on rat large-conductance Ca²⁺-activated K⁺ channel. *Biophys J* **86**:2871-2882.

Ha TS, Jeong SY, Cho SW, Jeon H, Roh GS, Choi WS and Park CS (2000) Functional characteristics of two BK_{Ca} channel variants differentially expressed in rat brain tissues. *Eur J Biochem* **267**:910-918.

Hamil OP, Marty A, Neher E, Sakmann B and Sigworth FJ (1981) Improved patch-clamp techniques for high-resolution current recording from cells and cell-free membrane patches. *Pflugers Arch* **391**:85-100.

Imaizumi Y, Sakamoto K, Yamada A, Hotta A, Ohya S, Muraki K, Uchiyama M and Ohwada T (2002) Molecular basis of pimarane compounds as novel activators of large-conductance Ca²⁺-activated K⁺ channel α -subunit. *Mol Pharmacol* **62**:836-846.

Jaggar JH, Porter VA, Lederer WJ and Nelson MT (2000) Calcium sparks in smooth muscle. *Am J Physiol Cell Physiol* **278**:C235-256.

Kaczorowski GJ and Garcia ML (1999) Pharmacology of voltage-gated and calcium-activated potassium channels. *Curr Opin Chem Biol* **3**:448-458.

Lawson K (2000) Is there a role for potassium channel openers in neuronal ion channel disorders? *Expert Opin Investig Drugs* **9**:2269-2280.

Liman ER, Tytgat J and Hess P (1992) Subunit stoichiometry of a mammalian K⁺ channel determined by construction of multimeric cDNAs. *Neuron* **9**:861-871.

Meera P, Wallner M, Jiang Z and Toro L (1996) A calcium switch for the functional coupling between alpha (hslo) and beta subunits (KV,Ca beta) of maxi K channels. *FEBS Lett*

382:84-88.

Meera P, Wallner M, Song M and Toro L (1997) Large conductance voltage- and calcium-dependent K^+ channel, a distinct member of voltage-dependent ion channels with seven N-terminal transmembrane segments (S0-S6), and extracellular N terminus and an intracellular (S9-S10) C terminus. *Proc Natl Acad Sci USA* **94**:14066-14071.

Ohi Y, Yamamura H, Nagano N, Ohya S, Muraki K, Watanabe M and Imaizumi Y (2001) Local Ca^{2+} transients and distribution of BK channels and ryanodine receptors in smooth muscle cells of guinea-pig vas deferens and urinary bladder. *J Physiol* **534**:313-326.

Pattern C, Thomson S. and Epel D (2004) Some precautions in using chelators to buffer metals in biological solutions. *Cell Calcium* **35**:427-431.

Qian X, Nimigean CM, Niu X, Moss BL and Magleby KL (2002) Slo1 tail domains, but not the Ca^{2+} bowl, are required for the β 1-subunit to increase the apparent Ca^{2+} sensitivity of BK channels. *J Gen Physiol* **120**:829-843.

Shieh CC, Coghlan M, Sullivan JP and Gopalakrishnan M (2000) Potassium channels: molecular defects, diseases, and therapeutic opportunities. *Pharmacol Rev* **52**:557-594.

Shipston MJ (2001) Alternative splicing of potassium channels: a dynamic switch of cellular excitability. *Trends Cell Biol* **11**:353-8.

Starrett JE, Dworetzky SI and Gibkoff VK (1996) Modulators of large-conductance calcium-activated potassium (BK) channels as potential therapeutic targets. *Current Pharmaceut Design* **2**:413-428.

Toro L, Wallner M, Meera P and Tanaka Y (1998) Maxi- K_{Ca} , a Unique member of the voltage-gated K^+ channel superfamily. *News Physiol Sci* **13**:112-117.

Valverde MA, Rojas P, Amigo J, Cosmelli D, Orio P, Bahamonde MI, Mann GE, Vergara C and Latorre R (1999) Acute activation of Maxi-K channels (hSlo) by estradiol binding to the beta subunit. *Science* **285**:1929-1931.

Vergara C, Latorre R, Marrion NV and Adelman JP (1998) Calcium-activated potassium channels. *Curr Opin Neurobiol* **8**:321-329.

Wallner M, Meera P and Toro L (1999) Molecular basis of fast inactivation in voltage and Ca^{2+} -activated K^{+} channels: a transmembrane β -subunit homolog. *Proc Natl Acad Sci USA* **96**:4137-4142.

Weiger TM, Hermann A and Levitan IB (2002) Modulation of calcium-activated potassium channels. *J Comp Physiol A Neuroethol Sens Neural Behav Physiol* **188**:79-87.

Xia XM, Ding JP and Lingle CJ (1999) Molecular basis for the inactivation of Ca^{2+} - and voltage-dependent BK channels in adrenal chromaffin cells and rat insulinoma tumor cells. *J Neurosci* **19**:5255-5264.

FOOTNOTES

This research was supported by research grants from Korea Science and Technology Foundation (R01-2002-000-00354-0) and the Ministry of Science and Technology of Korea (21C Frontier, 03K2201-00320) to C.-S. Park, and a grant from the Ministry of Health and Welfare (Korea Health 21 R&D Project, 0405-NS01-0704-0001-13) to Y.-C. Kim.

LEGENDS FOR FIGURES

Figure 1. Rapid and reversible activation of macroscopic rSlo channel currents by TBIC

Representative diary-plot of mean currents evoked by rSlo channels was shown as a continuous recording. Ionic currents were elicited every second with 50-ms step-pulses of 50 mV from the holding voltage of -100 mV. Currents were averaged for 3-ms in between 45 to 48-ms of voltage pulse. TBIC was superfused on extracellular side of patch membrane at $20\text{ }\mu\text{M}$ (*solid bar*). Each representative current trace (**a – d**) was obtained at the time indicated by arrows. *Inset*, chemical structure of TBIC, 7-trifluoromethyl-10*H*-benzo[4,5]furo[3,2-*b*]indole-1-carboxylic acid

Figure 2. Effects of β subunits on TBIC-dependent potentiation of macroscopic rSlo currents

Titration curves (*right panels*) of rSlo (**A**), rSlo/h β 1 (**B**), and rSlo/r β 4 channels (**C**) were shown with their representative raw-traces in various TBIC concentrations (*left panels*). Ionic currents were elicited with 50-ms step-pulses of 50 ms from a holding voltage of -100 mV. Concentrations of extracellular TBIC were as indicated and concentration of intracellular Ca^{2+} was fixed at $2\text{ }\mu\text{M}$. The half-effective concentration (EC_{50}) and Hill coefficient (n) were obtained by fitting the experimental data to a logistic function, $I_{\text{max}} - I = (I_{\text{max}} - I_0) / \{1 + ([\text{TBIC}] / EC_{50})^n\}$, derived from Hill equation, where I_0 and I_{max} represent the current in the absence of TBIC and the maximum current measured at $300\text{ }\mu\text{M}$, respectively. The statistical of means and standard errors were calculated using the values obtained from more than three independent experiments. While the titration curves of both extracellular (*filled circles*) and intracellular TBIC (*filled squares*) were shown for rSlo channel, only extracellular titrations were presented for rSlo/h β 1 (*filled triangles*) and rSlo/r β 4 (*filled diamond*). Each data point represents the mean \pm S.E.M of more than four independent recordings

Figure 3. Effects of TBIC on current-voltage and conductance-voltage relationships of macroscopic rSlo current

A. Effects of TBIC on the macroscopic current-voltage (*I-V*) relationship of rSlo in different $[Ca^{2+}]_i$. Representative current traces of macroscopic rSlo currents (*left panels*) and their *I-V* relationships (*right panels*) were shown for two different $[TBIC]_o$, 30 μM and 100 μM , and three different $[Ca^{2+}]_i$, Ca^{2+} -free (*top*), 1 μM (*middle*), and 5 μM (*bottom*). Ionic currents were elicited with 200-ms step-pulses of different voltage protocols: -30 mV to 200 mV in 10-mV increments at free-calcium, -80 mV to 150 mV at 1 μM $[Ca^{2+}]_i$, and -150 mV to 80 mV at 5 μM $[Ca^{2+}]_i$ from holding potentials of -50 mV, -100 mV, and -150 mV, respectively. Each data-point in *I-V* relationships represents the mean current value measured over 198 ± 1.5 ms of test pulses. While the filling of symbols represent different concentrations of Ca^{2+} , Ca^{2+} -free (*empty*), 1 μM (*half-filled*), and 5 μM (*filled*), the shape of symbols differentiates the concentration of TBIC, control or 0 μM (*square*), 30 μM (*circle*), and 100 μM (*triangle*).

B. Effects of TBIC on the conductance-voltage (*G/V*) relationships of macroscopic rSlo currents. Conductance values were obtained from peak tail-currents and normalized to the maximum conductance observed at 100 μM $[TBIC]_o$. Each symbol represents the conductance values obtained from four different $[TBIC]_o$, control or 0 μM (*square*), 10 μM (*circle*), 30 μM (*triangle*), 100 μM (*down triangle*) and from three different $[Ca^{2+}]_i$; Ca^{2+} -free (*empty*, $n = 6$), 1 μM (*half-filled*, $n = 4$), and 5 μM (*filled*, $n = 4$).

C. Effects of TBIC on half-activation voltage ($V_{1/2}$). Each data-point represents the mean value \pm SEM of $V_{1/2}$ values obtained by fitting independent data sets with Boltzmann function. Each symbol represents identical meaning as Fig. 3B.

Figure 4. Effect of TBIC on single rSlo channels.

A. Typical single-channel current recordings of rSlo channels were shown at different membrane voltages. The concentration of intracellular Ca^{2+} (pipette Ca^{2+} concentration) fixed at 2 μM . Ionic currents of single-channels in a patch of oocyte membrane were continuously recorded at different membrane voltages in the absence (*left panels*) and presence of 20 μM TBIC perfused on the extracellular side (*right panels*). Open and closed states were denoted with dashed lines and solid lines (denoted as C), respectively. **B.** Effects of TBIC on the single-channel conductance. The unitary current-amplitude determined at 2 μM intracellular Ca^{2+} in the absence (*open circles*, $n = 7$) or presence of 20 μM TBIC (*filled circles*, $n = 5$) was plotted as a function of the test voltages. Each data point was obtained from all-points amplitude histograms fitted with Gaussian function. The slope-conductance of rSlo channel was estimated by linear least square regression. **C.** Effects of TBIC on voltage-dependent open probability (P_o) of single rSlo channel. Relationship of open-probability against membrane voltages of single rSlo channel were plotted in the absence (*empty circles*, $n = 5$) or presence of 20 μM TBIC (*filled circles*, $n = 4$). Data points were individually fitted to Boltzmann equation (*solid lines*), and the slope factors were determined as 0.031 for control and 0.035 for TBIC-induced currents, respectively. The open-probability of single rSlo channel were determined at 2 μM $[\text{Ca}^{2+}]_i$.

Figure 5. Effect of TBIC on native BK_{Ca} channels from rat hippocampus pyramidal neuron

A. Representative current traces of neuronal BK_{Ca} channels, recorded in excised outside-out membrane, were shown in the absence and the presence of TBIC at different membrane voltages. The intracellular free Ca^{2+} concentration was fixed at 2 μM and extracellular TBIC was fixed at 20 μM . Closed state and different open states were marked as a *solid* line (denoted as ‘C’) and *dotted* lines, respectively. Four BK_{Ca} channels were in this particular patch. The time-dependent effects of TBIC on native BK_{Ca} channels were shown in continuous recordings (*upper panels*) and their P_o

changes were monitored (*lower* panels) at two different holding-voltages, 25 mV (**B**) and –25 mV (**C**). P_o values were calculated in 2-sec intervals and the exposed time to extracellular TBIC was shown as solid bar.

Figure 1

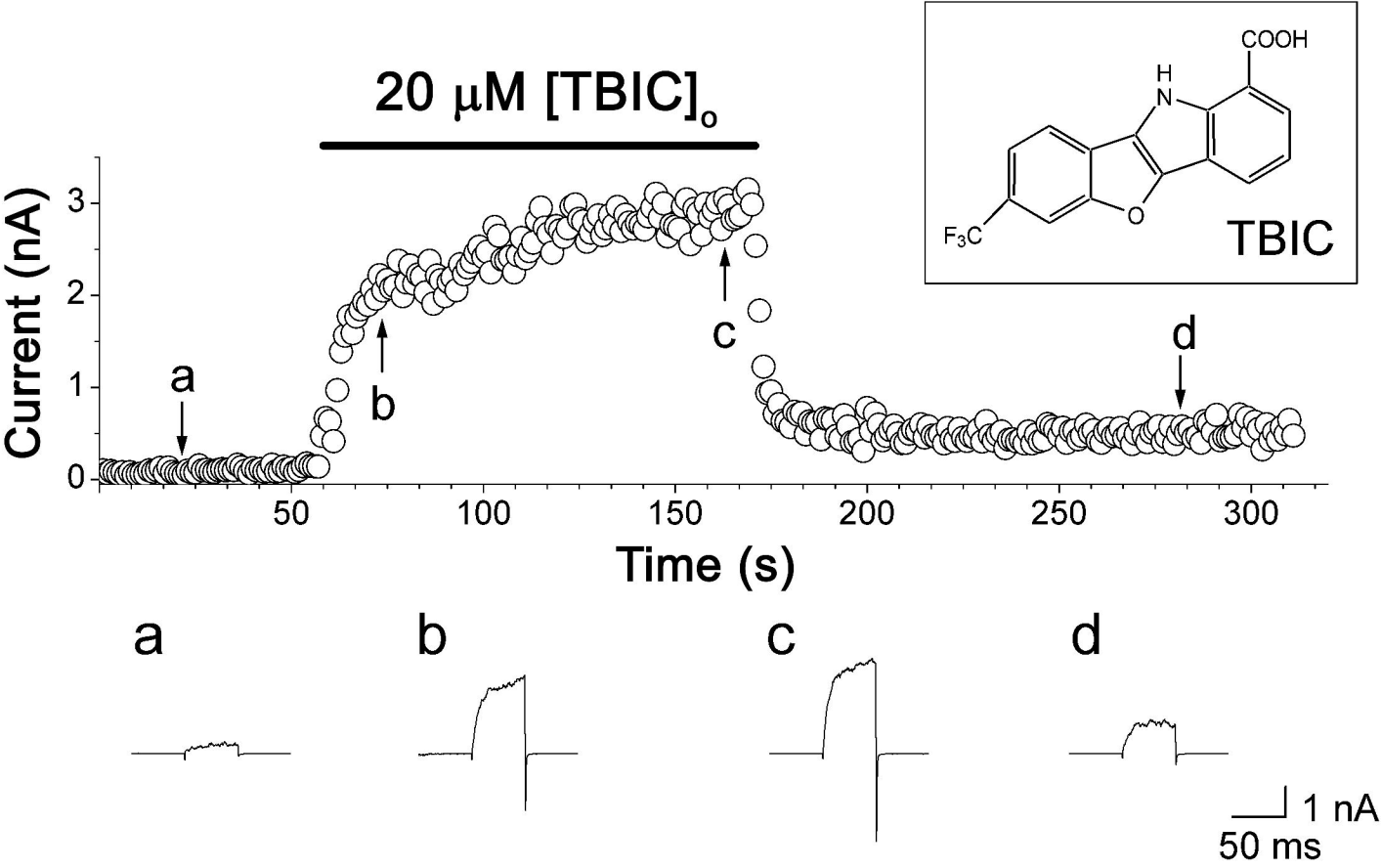


Figure 2

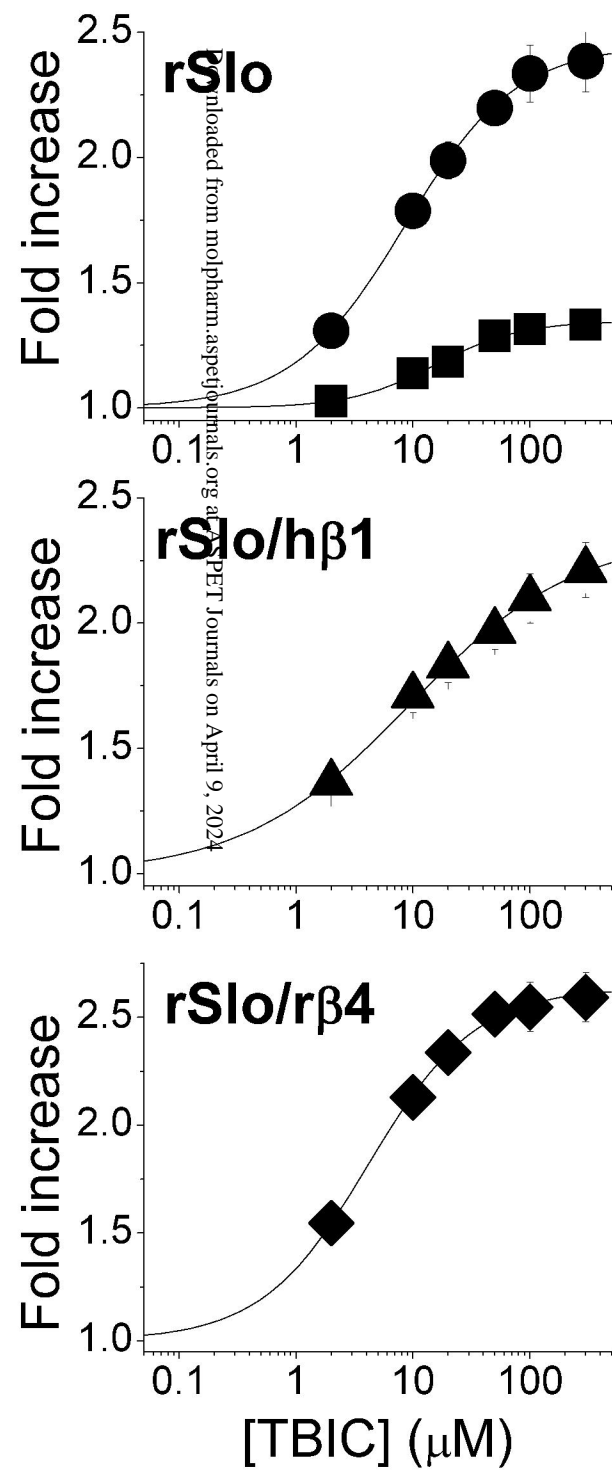
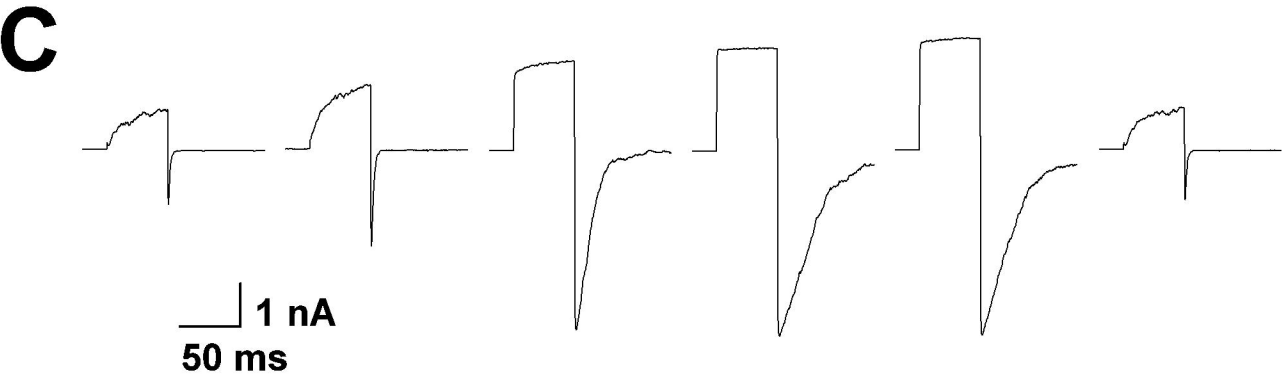
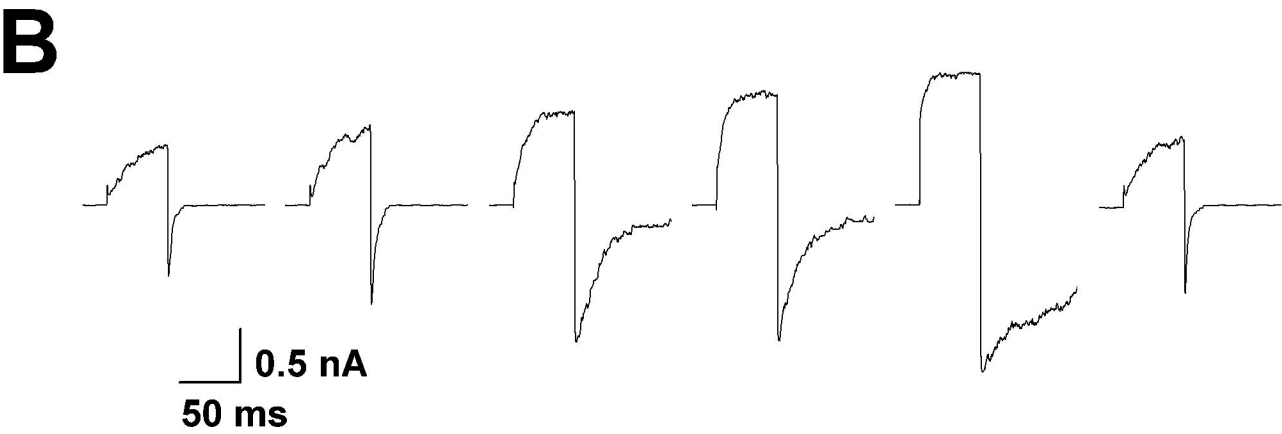
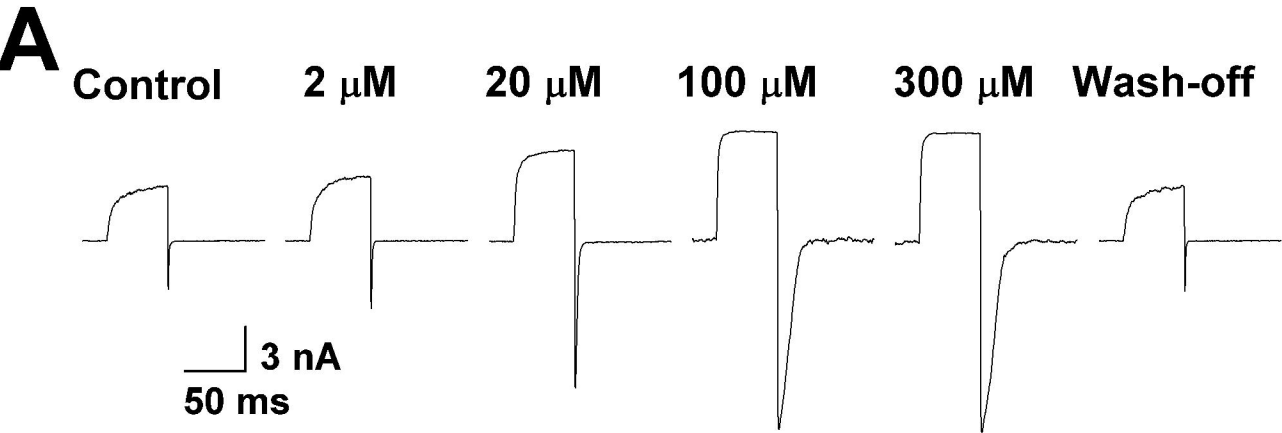


Figure 3

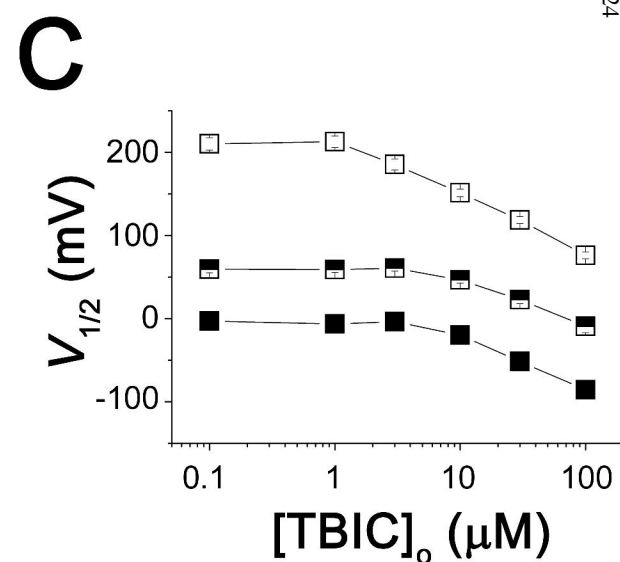
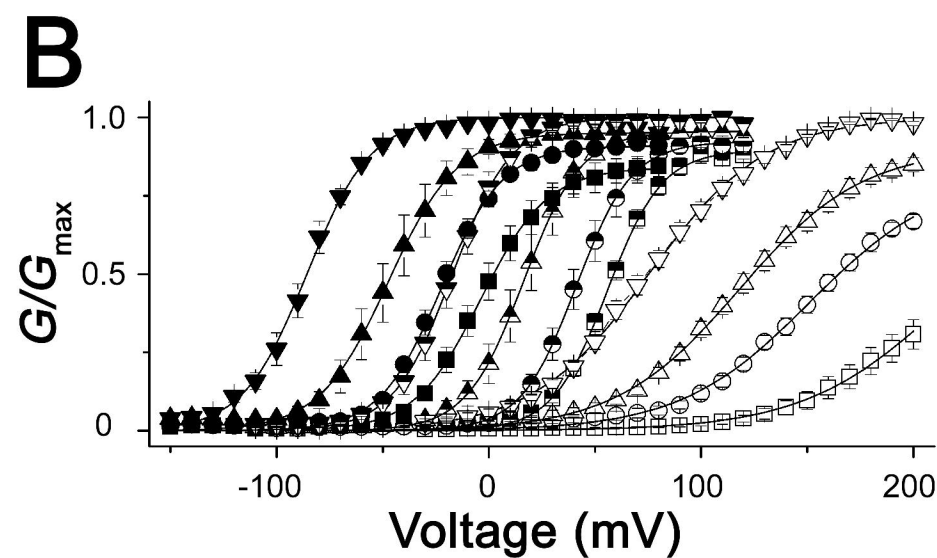
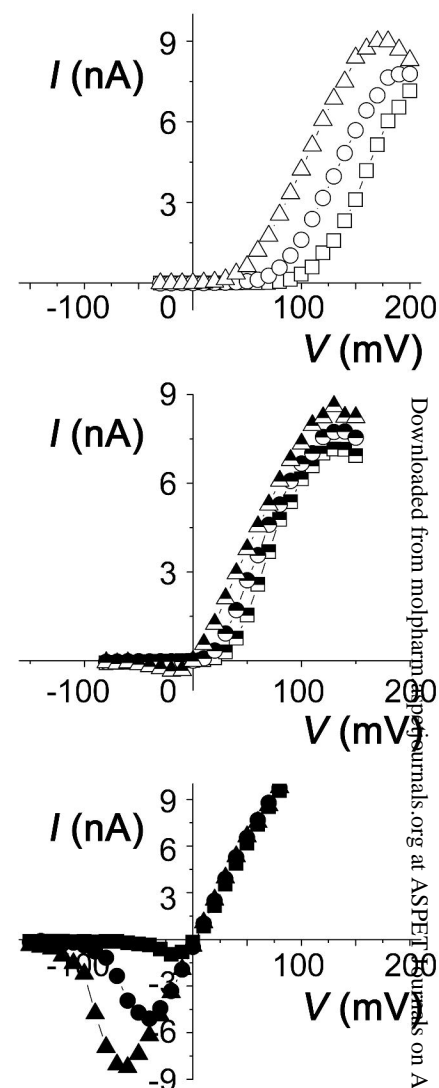
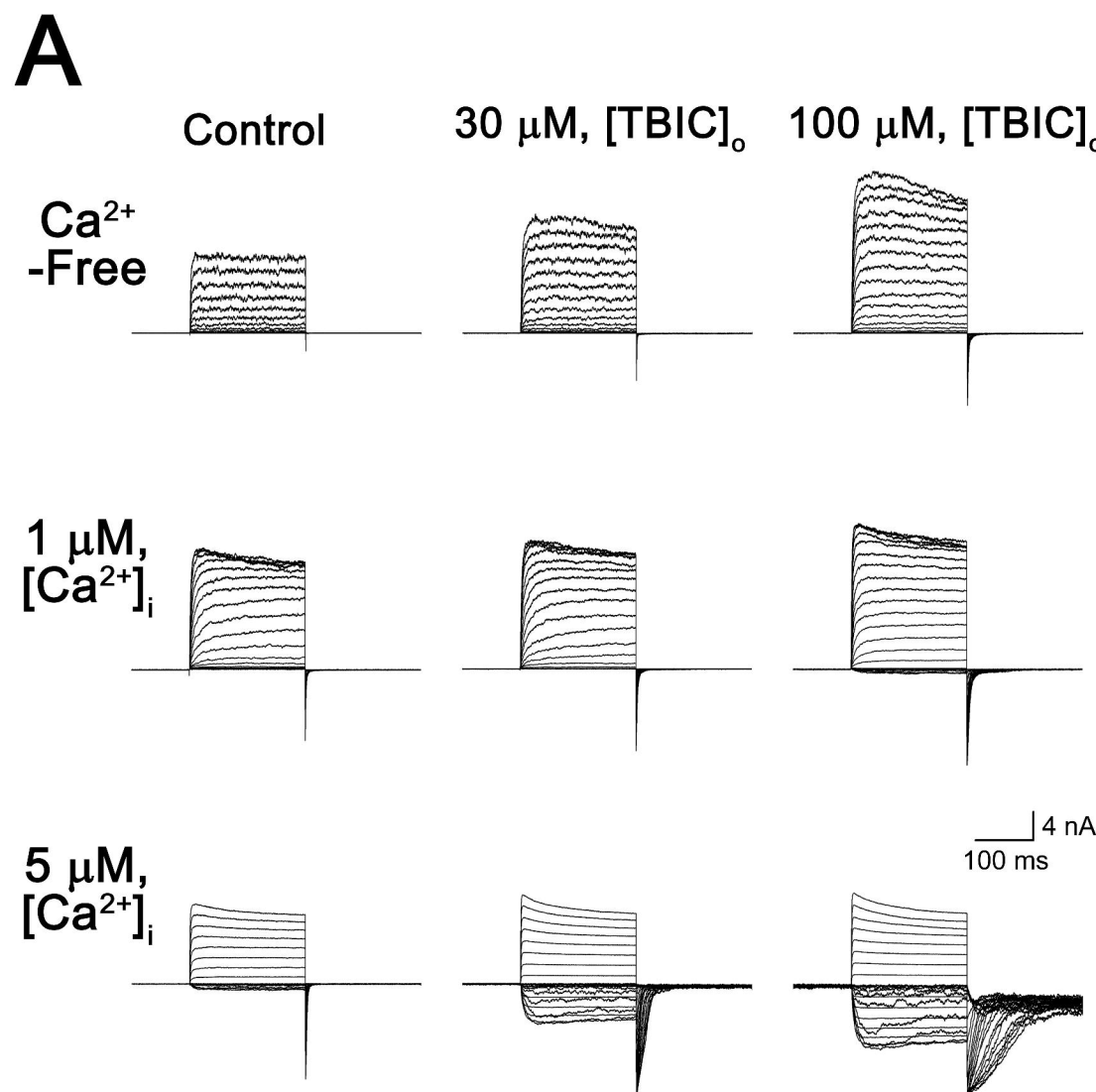


Figure 4

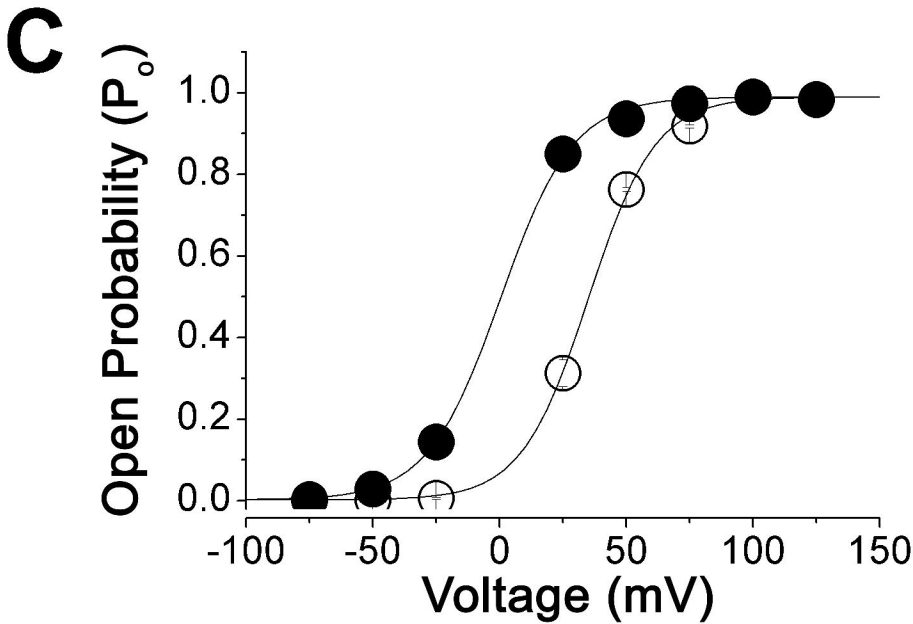
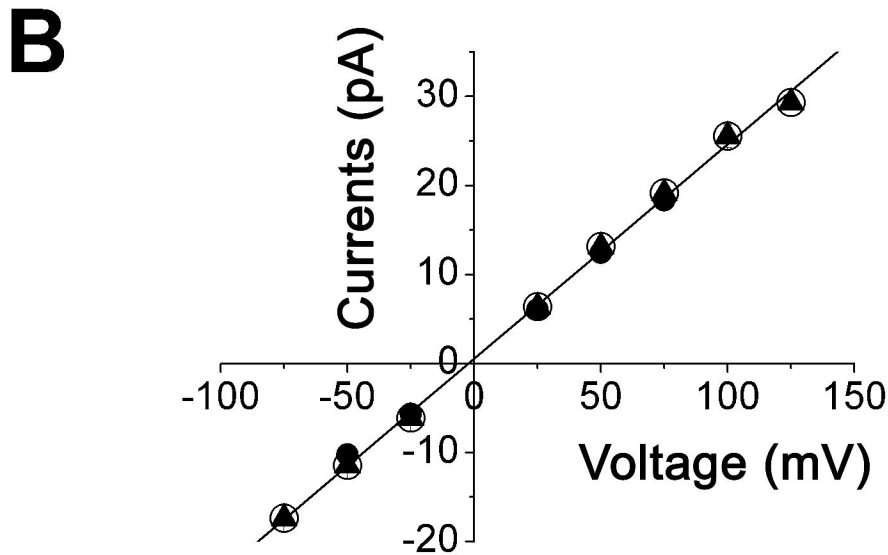
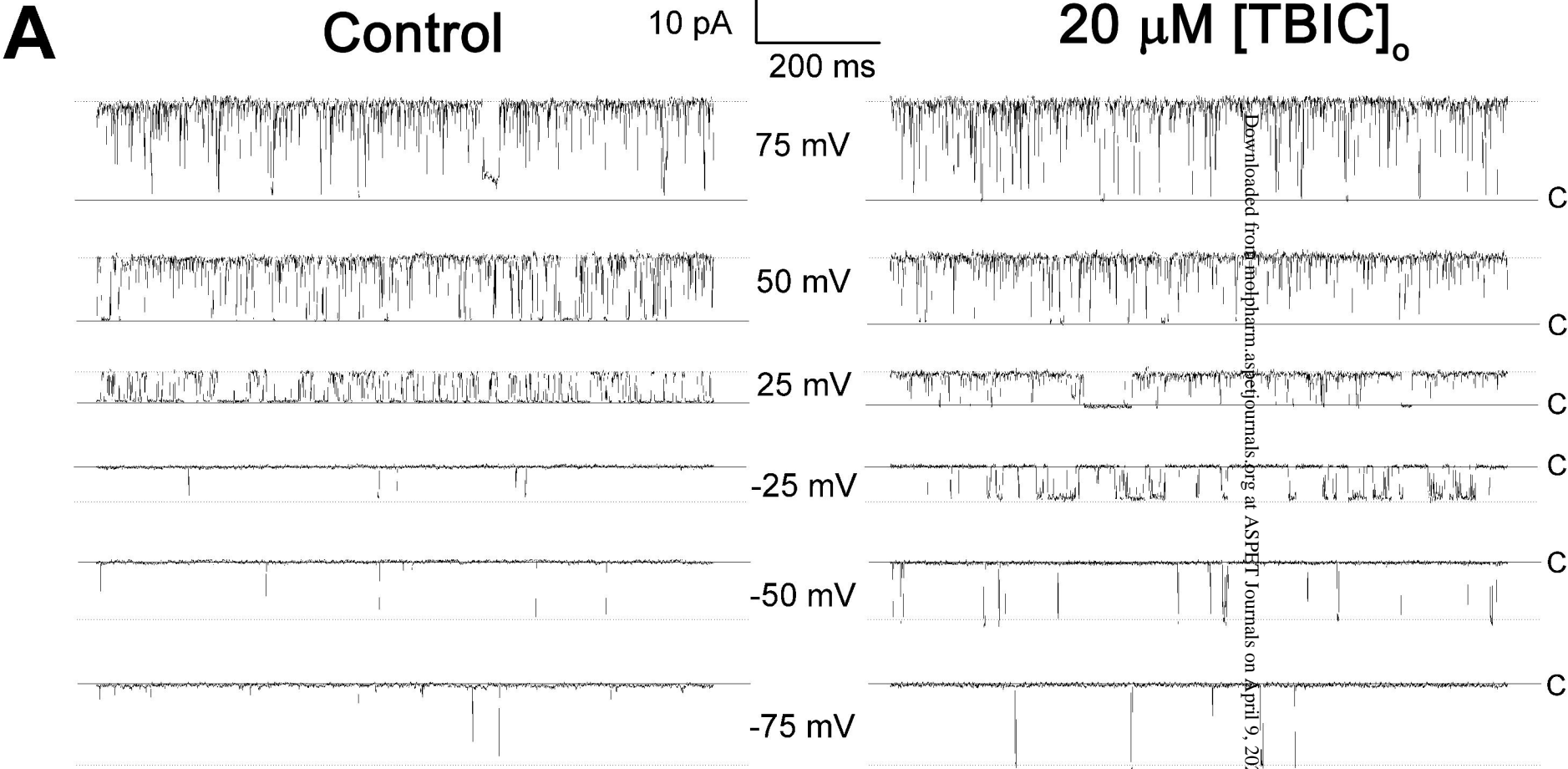


Figure 5

